HHS Public Access

Author manuscript

Cell Metab. Author manuscript; available in PMC 2017 August 09.

Published in final edited form as:

Cell Metab. 2016 August 9; 24(2): 269–282. doi:10.1016/j.cmet.2016.07.005.

Loss of NAD homeostasis leads to progressive and reversible degeneration of skeletal muscle

David W. Frederick[1], **Emanuele Loro**[2], **Ling Liu**[3,4], **Antonio Davila Jr.**[1], **Karthikeyani Chellappa**[1], **Ian M. Silverman**[5], **William J. Quinn 3rd**[1], **Sager J. Gosai**[5], **Elisia D. Tichy**[6], **James G. Davis**[1], **Foteini Mourkioti**[6], **Brian D. Gregory**[5], **Ryan W. Dellinger**[7], **Philip Redpath**[8], **Marie E. Migaud**[8], **Eiko Nakamaru-Ogiso**[9], **Joshua D. Rabinowitz**[3,4], **Tejvir S. Khurana**[2], and **Joseph A. Baur**[1]

[1]Department of Physiology and Institute for Diabetes, Obesity and Metabolism, Perelman School of Medicine, University of Pennsylvania, Philadelphia, Pennsylvania, 19104

[2]Department of Physiology and Pennsylvania Muscle Institute, Perelman School of Medicine, University of Pennsylvania, Philadelphia, Pennsylvania, 19104

[3]Lewis-Sigler Institute for Integrative Genomics, Princeton University, Princeton NJ 08544

[4]Department of Chemistry, Princeton University, Princeton NJ 08544

[5]Department of Biology, University of Pennsylvania, Philadelphia, Pennsylvania, 19104

[6]Department of Orthopaedic Surgery, Department of Cell and Developmental Biology, Perelman School of Medicine, University of Pennsylvania, Philadelphia, Pennsylvania, 19104

[7]ChromaDex Inc., Irvine, CA 92618

[8]John King Laboratory, School of Pharmacy, Queen's University Belfast, Belfast, UK

[9]Department of Biochemistry and Biophysics, Perelman School of Medicine, University of Pennsylvania, Philadelphia, Pennsylvania, 19104

Summary

NAD is an obligate co-factor for the catabolism of metabolic fuels in all cell types. However, the availability of NAD in several tissues can become limited during genotoxic stress and the course of natural aging. The point at which NAD restriction imposes functional limitations on tissue physiology remains unknown. We examined this question in murine skeletal muscle by specifically deleting Nampt, an essential enzyme in the NAD salvage pathway. Knockout mice exhibited a dramatic 85% decline in intramuscular NAD content, accompanied by fiber

To whom correspondence should be addressed: Dr. Joseph A. Baur, 3400 Civic Center Blvd, SCTR 12-114, Philadelphia, PA 19066, USA. Tel.: (215) 746-4585, Fax: (215) 898-5408, baur@mail.med.upenn.edu.

Author Contributions

DWF, EL, AD, FM, and JAB conceived experiments. DWF, EL, LL, AD, KC, ET, WJQ, and JGD performed experiments and analyzed data. IMS and SJG analyzed and visualized data. PR and MEM synthesized reagents. BDG, RWD, EN-O, JDR, and TSK provided expertise and feedback. DWF and JAB wrote the manuscript.

degeneration and progressive loss of both muscle strength and treadmill endurance. Administration of the NAD precursor nicotinamide riboside rapidly ameliorated functional deficits and restored muscle mass, despite having only a modest effect on the intramuscular NAD pool. Additionally, lifelong overexpression of Nampt preserved muscle NAD levels and exercise capacity in aged mice, supporting a critical role for tissue-autonomous NAD homeostasis in maintaining muscle mass and function.

Graphical Abstract

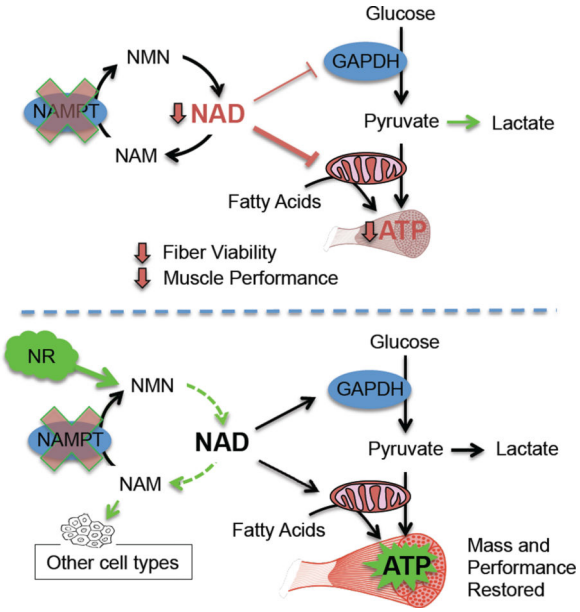

Introduction

The flow of carbon and energy through glycolysis and oxidative phosphorylation is dependent on the electron-shuttling nature of nicotinamide adenine dinucleotide (NAD), necessitating a tightly controlled balance between synthesis and degradation of this dinucleotide within the cell. NAD also serves as a co-substrate for enzymes that create signaling metabolites or post-translationally modify protein substrates. The resulting NAD-dependent signaling networks modify chromatin and transcription factor dynamics, as well as the kinetics of numerous enzymes, to coordinate physiological responses to circadian rhythms and feeding status (Asher and Sassone-Corsi, 2015). Accordingly, localized restrictions in NAD bioavailability could potentially have profound effects on cellular function by dampening these signals or impairing the production of ATP. Such restrictions have been reported during states of genotoxic stress that accompany a growing list of diseases, including cancer and neurodegeneration, as well as the course of natural aging (Cantó et al., 2015).

Since NAD contains a NAM moiety that cannot be synthesized by most tissues *de novo*, the vast majority of mammalian cells must instead rely on a salvage pathway to locally regenerate degraded NAD. An essential enzyme in this pathway, nicotinamide

phosphoribosyltransferase (Nampt), as well as its product, nicotinamide mononucleotide (NMN), are found in both intracellular and extracellular compartments, suggesting a systemic element to the salvage and distribution of NAD (Revollo et al., 2007a). With this in mind, recent strategies to globally augment the NAD salvage pathway in rodents have employed dietary supplementation of NAM-containing compounds, including NMN and nicotinamide riboside (NR). The latter compound can be phosphorylated by dedicated kinases to generate intracellular NMN through a Nampt-independent route (Bieganowski and Brenner, 2004). The multitude of physiological benefits stimulated by these vitamins, including enhanced oxidative metabolism, synaptic plasticity, and insulin sensitivity, has been attributed to increased NAD levels in tissues such as the liver, brain, and skeletal muscle (Cantó et al., 2012; Gong et al., 2013; Yoshino et al., 2011). However, the specific sites to which intact NAD precursors are distributed and utilized *in vivo* have not been demonstrated experimentally.

The concept of increasing NAD to gain a metabolic advantage inherently assumes that certain cells do not synthesize or access sufficient NAD to maintain optimal metabolic flux. This is proposed to be the case in aged rodents, which have been reported by multiple groups to exhibit decreases in the NAD content of brain, liver, and muscle, coincident with declines in the function of these tissues (Braidy et al., 2011; Gomes et al., 2013; Mouchiroud et al., 2013; Stein and Imai, 2014). In the case of skeletal muscle, a gradual decline in mass, strength, and oxidative capacity increases the susceptibility of the elderly to frailty and metabolic diseases. We have previously shown that NAD levels do not limit the cardiac and skeletal muscle physiology of young, healthy mice (Frederick et al., 2015). However, the lower threshold of NAD synthesis required to support NAD-dependent transcription and energetics in skeletal muscle has never been directly tested.

Here, we examine the consequences of restricting NAD availability in skeletal muscle by specific deletion of Nampt. We also examine the influence of the NAD precursor NR on muscle metabolism in states of compromised intramuscular NAD content. Our findings establish a lower threshold of tolerability for NAD loss in muscle and shed light on potential mechanisms driving the age-related declines in muscle function and metabolic capacity.

Results

Nampt-deficient muscle exhibits compromised energetics

To test the idea that deficits in intramuscular NAD may directly contribute to functional decline in skeletal muscle, we first attempted to generate mice with cardiac and skeletal muscle-specific deletion of *Nampt* using a floxed allele in combination with the same muscle creatine kinase (*ckmm*)-coupled Cre recombinase used previously to create Nampt transgenics (Frederick et al., 2015). To our surprise, only one female of the first 44 pups born to these crosses contained the homozygous deletion, suggesting predominant embryonic lethality. Reasoning that the low-level activity of *ckmm*-Cre in the heart may be responsible for the lethality, we instead crossed the floxed allele to a mouse line carrying Cre under control of the myosin light chain-1f promoter, which deletes exclusively in skeletal muscle (Bothe et al., 2000). These muscle-specific Nampt knockout (mNKO mice) appeared in the expected Mendelian ratios and had no obvious increase in mortality at the ages

studied. Muscles from mNKO mice are deficient in Nampt and contain <15% of the normal intramuscular concentrations of oxidized and reduced NAD by 3 months of age in both sexes (Figure 1A–C, S1A–C).

Muscle from mNKO mice exhibited a >60% decline in ATP content, clearly indicating energetic stress (Figure 1D). NAD is required by multiple enzymes involved in core metabolic pathways, including GAPDH in glycolysis and the three NAD-dependent dehydrogenases of the TCA cycle. To test whether mitochondrial ATP synthesis might be impaired by NAD restriction, we performed respirometry on the isolated organelles. While *in situ* compartment-specific quantitation of metabolites remains an outstanding challenge in the field, the concentrations of NAD retained in mitochondria post-isolation are postulated to reflect those existing in the tissue (Cantó et al., 2012). Consistently, we found mitochondria isolated from mNKO skeletal muscle to be depleted of NAD to a similar extent as whole muscle (Figure 1E) and inherently limited in their ability to utilize pyruvate and palmitoyl carnitine for respiration (Figure 1F, S1D). This limitation was not reflected in whole body respiration or feeding behavior, however, and correlated with only a trend toward decreased locomotion during the less active daylight hours (Figure 1G, H, S1E–G). At night, when energetic demands are higher, mNKO displayed an elevated respiratory exchange ratio (RER), indicating an decreased reliance on fatty acid oxidation compared to littermate controls (Figure 1I, S1H).

To test the ability of NAD-restricted muscle to perform under more demanding conditions, we conducted treadmill exercise tolerance tests. Surprisingly, mNKO mice aged 3 months appeared to fatigue at the same rate as littermate controls (Figure 1J). Nampt deficient mice were noted to be slightly smaller at this young adult age, apparently due to an overall reduction in lean mass (Figure 1K). However, this difference was not reflected in the weights of the major hindlimb muscles used for running (Figure 1L). We then tested contractile function *ex vivo* in isolated extensor digitorum longus (EDL) muscle by evoking contraction with direct electrical field stimulation. We found no change in the ability of mNKO muscles to generate force when a short stimulation was used to induce a single twitch contraction, yet significant declines in the force generated by repeated stimuli causing a sustained (tetanic) contraction (Figure 1M, N), suggesting that a primary functional impact of NAD loss is muscle weakness. A clinical hallmark of muscle weakness is decreased density and altered architecture of the bones to which muscles routinely apply tensile force. Upon examination of the tibial cortex by microcomputerized tomography (microCT), we found no significant decrease in bone mineral density, nor in the number or spacing of trabecular plates from 3-month-old mice (Figure S2C–E). However, decreased trabecular thickness, thought to contribute to age-related bone loss (Weinstein and Hutson, 1987), contributed to visibly rod-like trabecular morphology in mNKO tibias (Figure S2F, G).

mNKO mice develop myonecrosis and progressive loss of muscle function

We next investigated whether the observed muscle weakness in mNKO mice might have morphological correlates. Mutant hindlimb muscles showed an overall decrease in average fiber size accompanied by wider variability in this parameter, development of muscle stiffness, and a dramatic 8-fold increase in the appearance of centrally nucleated fibers,

indicative of recent regeneration (Figure 2A, B, S2A). The compromised membranes of myonecrotic patches that appeared in histological sections were confirmed by intraperitoneal administration of Evans blue dye (EBD), which visibly accumulated in the mNKO hindlimbs and localized to a minority of discrete fibers (Figure 2C). Thus, the energetic deficit in mNKO muscle parallels the loss and regeneration of individual fibers.

To determine if the mNKO myopathy worsened over time, as occurs in severe muscular dystrophies (Lu et al., 2014; Sacco et al., 2010), we monitored body weight and endurance as the animals aged. Though equal tibia lengths indicated that mutants were skeletally full grown (Figure S2B), the slight decrease in lean mass observed in 3-month-old male knockouts represented the beginning of a plateau in this parameter, driving a divergence in body weight as control littermates continued to gain weight (Figure 2D, E). By 7 months of age, the difference in muscle mass was apparent in the hindlimbs (Figure 2F). Females, which normally develop lean mass at a slower rate, exhibited no change in body weight. Upon exercise challenge, we found that 7-month-old mNKO mice could no longer maintain the treadmill performance of littermate controls (Figure 2G). Consistent with the *in vivo* performance, *ex vivo* twitch and tetanic force generation became severely limited by this age (Figure 2H, I), while immune cells appeared to increasingly infiltrate the endomysial space (Figure 2J). To further dissect the sequence of events leading to NAD-deficient myopathy, we examined electron micrographs of 7-month-old muscle and observed a clear pattern of discrete necrotic fibers in mNKO mice, often juxtaposed with fibers displaying remarkably normal sarcomeric and mitochondrial morphologies (Figure 2K). A minority of intermediate fibers exhibited swollen sarcoplasmic reticula, often associated with altered calcium homeostasis (Zhao et al., 2010), while others appeared only as remnants in the process of being cleared by multi-locular phagocytic immune cells (Figure 2K, bottom right).

To examine specific signaling pathways that might be linked to muscle wasting in mNKO mice, we performed whole transcriptome sequencing of mRNA isolated from quadriceps muscles. We were surprised to find fully 33% of detectable genes to be significantly altered in mNKO muscle, including those encoding 267 established transcription factors (Figure S3A, B, Table S1). We performed k-means clustering using all detected genes and found significant enrichment of those relating to muscle injury, inflammation, and immune response (cluster 4), while the most down-regulated cluster (3) corresponded to metabolic processes (Figure 3A, B). Interestingly, muscle-specific ubiquitin ligases MuRF1 (*Trim63*) and Atrogin1 (*Fbxo32*), associated with proteasome-dependent muscle wasting, were either unchanged or downregulated (Figure 3C). Nonetheless, expression of genes specific to muscle regeneration were highly enriched in the knockout (Figure 3D). In an attempt to isolate potential drivers of muscle-specific phenotypes in the context of immune infiltration, we performed Ingenuity Pathway Analysis (IPA) using a filter for muscle-associated transcripts (Table S1). Consistent with physiology, IPA identified increased expression of genes annotated for necrosis and muscle weakness and decreased expression of those relating to force generation and contractility (Figure S3C). The only consensus between top hits in the IPA and a *de novo* promoter motif analysis indicated that the mutant displayed reduced activity of signal transducer and activator of transcription 5b (Stat5b, Figure S3D,E, S4A), which mediates effects of growth hormone and androgens on postnatal muscle growth, but was not reported to impair fiber survival upon deletion (Klover et al., 2009).

Also of interest, the expression of p16ink4a (*Cdkn2a*), a gene strongly correlated with senescence and observed to increase in geriatric muscle satellite cells (Sousa-Victor et al., 2014), was dramatically up-regulated in the mutant, while additional overlap with age-related transcriptional changes was mild (Figure 3E, S3B). Moreover, we observed a striking overlap of differentially expressed genes with the *mdx* model of Duchene's Muscular Dystrophy (DMD) (Haslett et al., 2005), highlighting the extent of the muscle injury (Figure 3E).

Nicotinamide riboside functionally and morphologically restores NAD-deficient muscle

Metabolomic studies of NAD restriction in cancer cells and erythrocytes have shown that inhibition of glycolysis at the level of NAD-dependent glyceraldehyde 3-phosphate dehydrogenase (GAPDH) is primarily responsible for diminished ATP production (Hikosaka et al., 2014; Tan et al., 2013). Consistent with these reports, our metabolomic analysis indicated that substrates of GAPDH, as well as upstream intermediates of the pentose phosphate pathway (PPP), were significantly elevated in mNKO muscle (Figure 3F top, G). However, intermediates in the distal part of the glycolysis pathway and the TCA cycle were not detectably decreased *in vivo*, suggesting that mitochondrial function would not be limited by the supply of pyruvate. Thus, our data are inconsistent with the hypothesis that a block in glycolysis is the primary metabolic defect *in vivo*. We also noted that Nampt deletion did not result in the accumulation of its NAM substrate, but rather in a higher steady state concentration of methyl-NAM, an alternative fate for NAM equivalents.

The simple molecular basis of the defect in Nampt-deficient muscle led us to test whether the mNKO phenotypes might be reversed by augmenting the NAD salvage pathway via NAM-containing metabolites capable of entering the pathway downstream of Nampt. We first modeled this idea *in vitro* using differentiated C2C12 myotubes in the presence of the specific Nampt inhibitor FK866. The resulting metabolomic profile paralleled that of mNKO muscle (Figure 3H), but included decreases in distal glycolytic and TCA cycle intermediates, consistent with a more severe block in GAPDH activity (Figure 3F bottom). Using a [1,2-^{13}C]-glucose tracer, we confirmed an increase in the reverse aldolase reaction and a relative shift toward the non-oxidative arm of the PPP, as opposed to the NADP-dependent oxidative arm (Figure S4B, C). These findings are consistent with the buildup and interconversion of metabolites upstream of GAPDH. Importantly, these patterns were completely reversed following addition of 100 μM nicotinamide riboside (NR) to the culture media (Figure 3F bottom), indicating that NR can be directly utilized by myotubes to effectively bypass the requirement for Nampt activity.

To test whether NR-dependent NMN synthesis can bypass Nampt deficiency *in vivo*, we dissolved the compound in the drinking water to deliver an effective daily dose of ~400 mg/kg and confirmed that ~95% remained intact after one week. Mice beginning at age 5.5 months received the treatment continuously for 6 weeks. Intriguingly, this intervention appeared to completely prevent the development of exercise intolerance observed in 7-month-old mNKO mice and reversed lactic acidosis at the point of exhaustion (Figure 4A, B). Histological analysis confirmed that NR treatment induced muscle fiber remodeling in the mutant, partially restoring fiber diameter without affecting the degree of central

nucleation, which would not be expected to resolve in this time frame (Pastoret and Sebille, 1995) (Figure 4C). Consistent with these findings, we found that NR ameliorated the metabolic dysfunction of mitochondria isolated from mNKO muscle, completely restoring the maximal coupled respiration and muscle ATP content, despite a very small effect on total or mitochondrial NAD levels (Figure 4D–H). Interestingly, the changes in mitochondrial NAD appeared to correlate with respiratory capacity, reaching half-maximal respiration at ~0.5 nmol/mg of mitochondrial protein (Figure 4I). To test this relationship more directly, we depleted NAD from cultured myotubes using FK866 and titrated NR to obtain a range of mitochondrial NAD levels. Interrogation of NAD-dependent complex I relative to NAD-independent complex II again showed a steep dependence on NAD at the low end of the concentration range (Figure 4J), suggesting that the small changes in mitochondrial NAD content observed *in vivo* could be sufficient to confer functional benefits.

We next examined the ability of NR to reverse established muscular dysfunction by beginning a 6-week intervention in male knockout mice at 5.5 months of age, when loss of lean mass and endurance was already apparent. Consistent with rapid restoration of metabolic flux, mNKO mice experienced a complete restoration of exercise capacity after only one week, which persisted for the duration of the treatment (Figure 5A–D). We further demonstrated the near complete restoration of force generated by isolated mNKO muscles, as well as normalization of mass in all major hindlimb muscles, with no discernable effect of NR on littermate controls (Figure 5E–G). Whereas ATP levels in mNKO mice were nearly restored to those of wild type controls after NR treatment, we again found that NAD content of whole NR-treated mNKO muscle remained severely depleted, with only a trend toward improvement when compared to the untreated knockouts (Figure 5H, I).

Reasoning that poor bioavailability might be responsible for the weak impact of NR on steady state muscle NAD levels, we designed an isotope-labeled NR tracer, with a single ^{13}C and a single deuterium on the nicotinamide and ribose moieties, respectively, to elucidate the location and molecular form of its systemic distribution (Figure 6A). Direct incorporation of the tracer into NAD yields M+2 NAD, whereas breakdown and re-synthesis by the salvage pathway of any cell yields M+1 NAD (Figure 6B). We found that 100 minutes after oral administration, M+2 NAD was detectable in the liver, whereas the small fraction of NAD labeled in muscle was largely M+1 (Figure 6C, D). Accordingly, labeled NR was readily detectable in liver, but not in skeletal muscle (Figure 6E, F). Unlabeled NR was also detectable in both tissues and notably suppressed in mutant muscles, suggesting the existence of a naturally occurring pool capable of interconverting with NMN, perhaps mediated by 5’-nucleotidases (Grozio et al., 2013; Kulikova et al., 2015). The minute amount of dual-labeled NAD observed in muscle indicates that direct utilization of NR by the muscle does occur. However, oral NR dosing increased circulating NAM ~40-fold while NMN remained unchanged and NR was detected only at trace levels in the blood. Thus, the majority of the orally administered NR that reaches the muscle appears to enter in the form of liberated NAM or as NMN (Figure 6G, H).

To test whether NAM itself might account for some of the beneficial effects of NR treatment, we performed an additional experiment that included three weeks of NAM treatment. NAM-treated mice exhibited intermediate phenotypes with regard to muscle

performance and NAD levels (Figure S5A–I). We further assessed the ability of NR or NAM to stimulate the proliferation of muscle satellite cells in the mutant and found that proliferation trended lower, while the simultaneous appearance of Evans Blue positive fibers was dramatically reduced by both NR and NAM, confirming a reduction in fiber turnover in treated muscles (Figure S6A–E).

Gain of Nampt function maintains exercise capacity into old age

Following our earlier studies indicating little impact of Nampt overexpression in cardiac and skeletal muscle of young mice (Frederick et al., 2015), we decided to examine the effect of lifelong muscle-specific Nampt transgene expression (mNTG mice) near the end of the expected mouse lifespan at 24 months of age (Figure 7A). When compared to young adult cohorts, aged controls exhibited reductions in intramuscular NAD of approximately one third, in line with previous reports (Figure 7B). While transgenic mice also exhibited a decline with age, the higher starting point rendered intramuscular NAD levels in aged mNTG mice indistinguishable from that of young controls. Interestingly, aged mNTG mice exhibit a moderate reduction in body weight (Figure 7C) and marked improvement in exercise capacity, closer to the performance of young mice than to that of the age-matched controls (Figure 7D, E). To determine whether the enhanced exercise capacity was secondary to the induction of an NAD-dependent transcriptional program in muscle, we performed whole-transcriptome sequencing of mRNA from quadriceps muscle. To our surprise, only 18 of the more than 15,000 detected genes were significantly altered by the transgene when compared to age-matched 24-month-old controls, even using relaxed selection criteria (Figure 7F, Table S2). From these, no obvious candidates for regulation of oxidative metabolism emerged. Furthermore, the age-related changes in gene expression in the mNTG generally mirrored those of controls, significantly overlapping in 87 instances and opposing in none (Figure 7G, H, Table S2). The lack of strong transcriptional changes favors the model that Nampt overexpression prevents age-related decline in muscle function through a direct metabolic mechanism: by facilitating glycolytic and TCA cycle flux.

Discussion

To better understand the physiological and therapeutic implications of altering NAD metabolism within skeletal muscle, we created a model of primary pyridine nucleotide deficiency using a floxed allele of *Nampt*. Our finding that the NAD content of muscle was decreased by ~85% confirmed the prevailing view that the salvage route of NAD synthesis from NAM sustains the vast majority of the NAD utilized by this tissue. Neither the natural abundance of circulating NMN, nor extracellular Nampt (eNampt) (Revollo et al., 2007b) appear sufficient to alleviate the resulting pathology, indicating that muscle NAD metabolism is largely an isolated system. Nonetheless, our observation that mNKO mice appear grossly unaffected for several weeks post-weaning illustrates the incredible metabolic flexibility of skeletal muscle and supports the proposition that intramuscular NAD of young wildtype mice is maintained at a level far in excess of that absolutely required for muscle function.

Given the essential nature of NAD in bioenergetics, there must exist a threshold below which cells depleted of this metabolite experience an energetic crisis. Despite the normal structural features of many fibers in mNKO mice, the loss of energy charge from adenine nucleotides in their muscles suggest that they are approaching this threshold. Pharmacological inhibition of Nampt in cultured tumor cells has been found to restrict glycolytic flux at the level of GAPDH, the only NAD-dependent enzyme in this pathway, creating a signature increase in the prevalence of upstream metabolites and depletion of downstream metabolites (Tan et al., 2013). We observed a closely related pattern in cultured myotubes treated with FK866. Accumulation of upstream metabolites, but not depletion of downstream metabolites, was also apparent *in vivo*, supporting the proposal of Tan and colleagues that concentrations of proximal glycolytic intermediates in biopsied tissue samples may have clinical utility as biomarkers of severe NAD restriction (Tan et al., 2013). However, the lack of depletion of downstream metabolites and occurrence of lactic acidosis upon running the mNKO animals to exhaustion suggest that the main cause of impaired ATP production is lower mitochondrial, not glycolytic, flux. Indeed, in the face of low NAD, elevated levels of upstream glycolytic intermediates may help maintain flux through GADPH and thus glycolysis. It is noteworthy that a previously reported model of skeletal muscle cytochrome c oxidase deficiency was found to survive as long as four months, despite near complete deficiency in mitochondrial function (Diaz, 2005), indicating that glycolysis alone can support a substantial portion of the energetic burden in youthful muscle.

Though isolated disturbances in NAD synthesis are uncommon in nature, the impairment of ATP production observed in the mNKO mice is a characteristic feature of metabolic myopathies, which include numerous muscle wasting syndromes modeled in mice and stemming from inborn errors of metabolism (Cerutti et al., 2014; Diaz, 2005; Graham et al., 1997). A key similarity between these models and the phenotypes of mNKO mice is the progressive decline in muscle contractile function over weeks or months, accompanied by altered myofibrillar morphology. Unlike most myopathies, however, the death of mNKO muscle fibers occurs in the absence of any upregulation of the catabolic ubiquitin ligases Atrogin1 or MuRF1, implicating a largely unregulated mechanism of cell death. Rather, this pattern mirrors the well-documented mechanism of poly(ADP) ribose polymerase-mediated cell death, in which rapid NAD consumption restricts intracellular ATP to a level below that required by the apoptotic program, instead promoting necrosis (Ha and Snyder, 1999). Our histology and electron microscopy provide evidence consistent with this mechanism. Transcriptionally, there is a striking resemblance between mNKO muscle and that of the well-characterized *mdx* model of DMD. This observation was unexpected, given that the former defect is strictly metabolic and the latter strictly structural, and especially compelling in light of reports that *mdx* muscle contains less NAD than that of age-matched controls and appears limited in aerobic capacity by complex I (Chalkiadaki et al., 2014; Rybalka et al., 2014). NAD supplementation also counteracts at least one additional laminopathy modeled in zebrafish (Goody et al., 2012). Thus, our finding that muscle fiber atrophy can be derived solely from disrupted NAD salvage raises the intriguing possibility that NAD loss contributes to the etiology of at least a subset of established muscular dystrophies.

Our finding that a single week of NR supplementation was sufficient to dramatically restore exercise capacity in mNKO mice points to restoration of muscle metabolic flux as a likely

mechanism. Indeed, the muscle remodeling necessary to increase oxidative capacity by training typically requires weeks to months. While NR could conceivably contribute to the endurance phenotype through a variety of effects in other tissues, our *ex vivo* experiments favor a model that is primarily muscle fiber-autonomous. The persistent restoration of peak twitch and tetanic force in isolated muscles indicates that the effect is not strictly dependent on the neuromuscular junction or the acute supply of circulating metabolic substrates. Similarly, the restored oxidative capacity of mitochondria persists post-isolation, suggesting a direct effect on the metabolic capacity of muscle fibers.

In light of its potent phenotypic effects in mNKO mice, we were surprised to find that NR exerts only a subtle influence on the steady state concentration of NAD in muscles. Our tracer studies suggest that this is largely attributable to breakdown of orally delivered NR into NAM prior to reaching the muscle. Nonetheless, our results indicate that NR is more effective than NAM for reversing mNKO phenotypes (Figure S5). The correlation between the NAD content and the respiratory capacity of isolated mitochondria, even in cultured myotubes (Figure 4), supports the model that subtle changes in NAD can disproportionately modulate aerobic metabolism. It is important to note that NAD turnover may vary independently from NAD concentration and that small changes in average tissue concentration might reflect larger changes in specific cells or subcellular compartments. It is also possible that intramuscular conversion of NAD into secondary messengers potently influences calcium homeostasis, which is both essential to muscle contraction and can independently modulate mitochondrial respiration (Cárdenas et al., 2010).

Our results leave open the possibility that some of the functional improvements in NR-treated mNKO muscles are secondary to effects in other cell types. Because necrosis was decreased by both NR and NAM at the time point examined in our study, the net effect on the regenerative capacity of satellite cells is not clear, and will be an important focus of future work. The observation that NAM treatment was sufficient to confer a partial effect in mNKO muscle supports the model that effects outside of differentiated fibers contribute to the benefits of NR. Such indirect activities may help to explain how oral NR administration clearly mitigates the severity of insults to a growing list of tissues in which robust NAD decrements were not observed before treatment (Brown et al., 2014; Cerutti et al., 2014; Khan et al., 2014; Xu et al., 2015). We also cannot exclude the possibility that NAM contributes slightly to the NAD pool in mNKO myofibers by inhibition of NAM-sensitive NAD-consumers or via residual Nampt activity in fibers or fusing myoblasts.

An important goal of this work was to determine whether primary NAD deficiency could mimic age-associated physiological decline in muscle function. We were intrigued to find the expression of *Cdkn2a*, encoding the mitotic checkpoint inhibitor commonly known as p16ink4a, dramatically upregulated in mNKO muscle, since this biomarker of senescence is closely associated with aging in many tissues, including muscle (Krishnamurthy et al., 2004). Yet, while mNKO mice clearly exhibited progressive weakness and loss of both endurance and bone structure, the decline in NAD was more severe than has been observed for normal aging. Furthermore, the transcriptional signature predominately reflected the muscle regeneration and immune infiltration, making it difficult to assess whether more subtle features of aging were emergent. In this regard, the overexpression model offers

important insights. Complementary to our results in mNKO mice, preventing the natural decline of intramuscular NAD in 24-month-old mNTG mice significantly improved exercise capacity as compared to littermate controls. Interestingly, transcriptome analysis indicated that this improvement is not secondary to any major changes in gene expression, suggesting a model in which metabolic flux and/or NAD-dependent post-translational modifications play a major role. The implication that the modest age-related decline in NAD can have functional consequences is in stark contrast to the ability of young mice to initially tolerate a much more severe depletion, and suggests that one or more additional factors may aggregate over time to exacerbate the dependence of muscle function on internal NAD stores. Alternatively, the aggregate decline in NAD with age may be driven by a subset of fibers with more severe depletion.

The mechanisms by which Nampt overexpression can restore function in aged, and perhaps dystrophic muscle will be an important area for future investigations, while the mNKO model may prove useful for resolving the efficacy of novel therapeutics designed to enhance muscle NAD content. Overall, our results clearly indicate that Nampt expression is critical to the maintenance of both the mass and contractile function of skeletal muscle, lending support to the idea that loss of NAD homeostasis may contribute to genetic and age-related causes of physiological decline in this tissue.

Experimental procedures

Generation of transgenic animals

Mice deficient for *Nampt* in skeletal muscle were generated by crossing Nampt$^{fl/fl}$ mice (Rongvaux et al., 2008) to mice carrying Cre under control of the myosin light chain 1f (Mlc1f) promoter (Bothe et al., 2000). Mice homozygous for the *Nampt* transgene under expression of *ckmm*-Cre were generated as described previously (Frederick, 2015). All mice were on a C57BL6 background, housed in a temperature-controlled pathogen-free barrier facility on a 12 hour/12 hour light/dark, fed a standard chow diet (Rodent Diet 5010, LabDiet), and provided water chlorinated at 2–4 ppm according to approved Institutional Animal Care and Use Committee protocols.

NR and NAM administration

NR chloride or NAM were dissolved weekly in the drinking water at 12 mM, sterile filtered, and provided *ad libitum* in light-protected bottles. For NR^{M+2} experiments, custom synthesized isotopologue was dissolved in drinking water at 85 mM and administered to fed mice at a dose of 200 mg/kg by oral gavage. Tail vein blood was sampled every 20 minutes until 100 minutes, at which time animals were sacrificed and tissues were snap frozen for metabolomics analysis.

NAD and ATP measurement

NAD was extracted from ~50 mg of snap frozen muscle tissue and 100 μg of purified muscle mitochondria in 0.5 mL and 0.1 mL of ice-cold 0.6 M perchloric acid, respectively. NAD content of extracts was measured using an enzymatic cycling assay and, for tissue samples, verified by HPLC, as described (Frederick et al., 2015). ATP was measured in neutralized

acid extracts using the ATP Determination Kit (Life Technologies) according to manufacturer instructions.

Mitochondrial isolation

Mitochondria were isolated from fresh triceps brachii muscles as reported previously (Frederick et al., 2015). Briefly, muscles were minced in ice-cold muscle homogenization buffer (100mM KCl, 50mM Tris-HCl, 5mM $MgCl_2$, 1mM EDTA, and 1.8mM ATP, pH 7.2), digested with 60 U/mL of protease from *Bacillus lichenformis* (Sigma, P5380), and further lysed with a Potter Elvehjem homogenizer for 10 minutes at 150 rpm. The homogenate was centrifuged twice at 720 ×g for 5 minutes before supernatants were combined and spun at 10,000 ×g for 20 minutes. The concentration of the final mitochondrial pellet was normalized in resuspension buffer (225mM sucrose, 44mM KH_2PO_4, 12.5mM Mg-acetate, and 6mM EDTA; pH 7.4) and immediately extracted for NAD measurement or used for respiration assays.

Mitochondrial respiration assays

Respiration of 15 μg of freshly isolated mitochondria was measured in MiRO5 respiration medium (110mM Sucrose, 20mM HEPES, 10mM KH_2PO_4, 20mM Taurine, 60mM K-lactobionate, 3mM $MgCL_2$•$6H_20$, 0.5mM EGTA, 1g/L defatted BSA, pH 7.2) using a Clark-type electrode (Strathkelvin Instruments, North Lanarkshire, Scotland) at 37°C. All chemicals were obtained from Sigma. Sequential addition of 5 mM malate, followed by either 10 mM pyruvate or 20 μM palmitoyl carnitine, were provided as substrates and 4 μmol of ADP were added to stimulate maximal coupled respiration. Maximal uncoupled respiration was measured following addition of 2 μg/mL oligomycin from and 4 μM carbonilcyanide *p*-triflouromethoxyphenylhydrazone (FCCP). Assays were ended by the addition of 5 μM antimycin A to cease respiration.

Statistical Analyses

Comparisons of two groups were performed using two-tailed paired or unpaired Student's t-test, as indicated. Comparisons of three or more groups were performed using one-way ANOVA followed by Tukey's or Dunnett's post-hoc test, as indicated. Significance was defined as $p<0.05$. For individual metabolites within metabolomic data sets, the nominal statistical significance is reported based on Student's t-test. Non-linear least-squares regressions were fit to a rectangular hyperbola according to the equation $Y=\frac{V_{\max}\cdot[NAD]}{K_m+[NAD]}$, where V_{max} and K_m are determined by the rate-limiting enzyme, using Graphpad Prism 5 software. Statistical methods related to RNAseq analysis are provided in the Supplemental Information and all sequencing data generated in this study have been deposited to the USCS genome browser and GEO under the accession number GSE74570.

Supplementary Material

Refer to Web version on PubMed Central for supplementary material.

Acknowledgments

We wish to thank M. Neinast, and J. Gong for technical assistance, C. Franzini-Armstrong and K-J. Won for expert advice, and all members of the Baur lab for feedback and suggestions. This work was supported by grants from the National Institutes of Health (R01 AG043483 and R01 DK098656 to J.A.B.). We thank the University of Pennsylvania Diabetes Research Center (DRC) for the use of the Biomarkers, Next-Generation Sequencing, and Mouse Metabolic Phenotyping, and Metabolism Cores (P30-DK19525), W-J. Tseng and the Penn Center for Musculoskeletal Disorders (P30-AR050950), J. Tobias and the Genomic Analysis Core, and R. Meade of the Electron Microscopy Core. R.W.D. is an employee and stockholder of Chromadex Inc., which manufactures and distributes NR.

References

Asher G, Sassone-Corsi P. Time for Food: The Intimate Interplay between Nutrition, Metabolism, and the Circadian Clock. Cell. 2015; 161:84–92. [PubMed: 25815987]

Bieganowski P, Brenner C. Discoveries of nicotinamide riboside as a nutrient and conserved NRK genes establish a Preiss-Handler independent route to NAD+ in fungi and humans. Cell. 2004; 117:495–502. [PubMed: 15137942]

Bothe GW, Haspel JA, Smith CL, Wiener HH, Burden SJ. Selective expression of Cre recombinase in skeletal muscle fibers. Genes. N. Y. N. 2000; 26:165–166. 2000.

Braidy N, Guillemin GJ, Mansour H, Chan-Ling T, Poljak A, Grant R. Age related changes in NAD+ metabolism oxidative stress and Sirt1 activity in wistar rats. PloS One. 2011; 6:e19194. [PubMed: 21541336]

Brown KD, Maqsood S, Huang J-Y, Pan Y, Harkcom W, Li W, Sauve A, Verdin E, Jaffrey SR. Activation of SIRT3 by the NAD+ Precursor Nicotinamide Riboside Protects from Noise-Induced Hearing Loss. Cell Metab. 2014; 20:1059–1068. [PubMed: 25470550]

Cantó C, Houtkooper RH, Pirinen E, Youn DY, Oosterveer MH, Cen Y, Fernandez-Marcos PJ, Yamamoto H, Andreux PA, Cettour-Rose P, et al. The NAD(+) Precursor Nicotinamide Riboside Enhances Oxidative Metabolism and Protects against High-Fat Diet-Induced Obesity. Cell Metab. 2012; 15:838–847. [PubMed: 22682224]

Cantó C, Menzies KJ, Auwerx J. NAD+ Metabolism and the Control of Energy Homeostasis: A Balancing Act between Mitochondria and the Nucleus. Cell Metab. 2015; 22:31–53. [PubMed: 26118927]

Cárdenas C, Miller RA, Smith I, Bui T, Molgó J, Müller M, Vais H, Cheung K-H, Yang J, Parker I, et al. Essential Regulation of Cell Bioenergetics by Constitutive InsP3 Receptor Ca2+ Transfer to Mitochondria. Cell. 2010; 142:270–283. [PubMed: 20655468]

Cerutti R, Pirinen E, Lamperti C, Marchet S, Sauve AA, Li W, Leoni V, Schon EA, Dantzer F, Auwerx J, et al. NAD(+)-Dependent Activation of Sirt1 Corrects the Phenotype in a Mouse Model of Mitochondrial Disease. Cell Metab. 2014

Chalkiadaki A, Igarashi M, Nasamu AS, Knezevic J, Guarente L. Muscle-Specific SIRT1 Gain-of-Function Increases Slow-Twitch Fibers and Ameliorates Pathophysiology in a Mouse Model of Duchenne Muscular Dystrophy. PLoS Genet. 2014; 10:e1004490. [PubMed: 25032964]

Diaz F. Mice lacking COX10 in skeletal muscle recapitulate the phenotype of progressive mitochondrial myopathies associated with cytochrome c oxidase deficiency. Hum. Mol. Genet. 2005; 14:2737–2748. [PubMed: 16103131]

Frederick DW, Davis JG, Dávila A, Agarwal B, Michan S, Puchowicz MA, Nakamaru-Ogiso E, Baur JA. Increasing NAD synthesis in muscle via nicotinamide phosphoribosyltransferase is not sufficient to promote oxidative metabolism. J. Biol. Chem. 2015; 290:1546–1558. [PubMed: 25411251]

Gomes AP, Price NL, Ling AJY, Moslehi JJ, Montgomery MK, Rajman L, White JP, Teodoro JS, Wrann CD, Hubbard BP, et al. Declining NAD(+) induces a pseudohypoxic state disrupting nuclear-mitochondrial communication during aging. Cell. 2013; 155:1624–1638. [PubMed: 24360282]

Gong B, Pan Y, Vempati P, Zhao W, Knable L, Ho L, Wang J, Sastre M, Ono K, Sauve AA, et al. Nicotinamide riboside restores cognition through an upregulation of proliferator-activated

receptor-γ coactivator 1α regulated β-secretase 1 degradation and mitochondrial gene expression in Alzheimer's mouse models. Neurobiol. Aging. 2013; 34:1581–1588. [PubMed: 23312803]

Goody MF, Kelly MW, Reynolds CJ, Khalil A, Crawford BD, Henry CA. NAD+ Biosynthesis Ameliorates a Zebrafish Model of Muscular Dystrophy. PLoS Biol. 2012; 10:e1001409. [PubMed: 23109907]

Graham BH, Waymire KG, Cottrell B, Trounce IA, MacGregor GR, Wallace DC. A mouse model for mitochondrial myopathy and cardiomyopathy resulting from a deficiency in the heart/muscle isoform of the adenine nucleotide translocator. Nat. Genet. 1997; 16:226–234. [PubMed: 9207786]

Grozio A, Sociali G, Sturla L, Caffa I, Soncini D, Salis A, Raffaelli N, De Flora A, Nencioni A, Bruzzone S. CD73 protein as a source of extracellular precursors for sustained NAD+ biosynthesis in FK866-treated tumor cells. J. Biol. Chem. 2013; 288:25938–25949. [PubMed: 23880765]

Ha HC, Snyder SH. Poly(ADP-ribose) polymerase is a mediator of necrotic cell death by ATP depletion. Proc. Natl. Acad. Sci. U. S. A. 1999; 96:13978–13982. [PubMed: 10570184]

Haslett JN, Kang PB, Han M, Kho AT, Sanoudou D, Volinski JM, Beggs AH, Kohane IS, Kunkel LM. The influence of muscle type and dystrophin deficiency on murine expression profiles. Mamm. Genome Off. J. Int. Mamm. Genome Soc. 2005; 16:739–748.

Hikosaka K, Ikutani M, Shito M, Kazuma K, Gulshan M, Nagai Y, Takatsu K, Konno K, Tobe K, Kanno H, et al. Deficiency of Nicotinamide Mononucleotide Adenylyltransferase 3 (Nmnat3) Causes Hemolytic Anemia by Altering the Glycolytic Flow in Mature Erythrocytes. J. Biol. Chem. 2014; 289:14796–14811. [PubMed: 24739386]

Khan NA, Auranen M, Paetau I, Pirinen E, Euro L, Forsström S, Pasila L, Velagapudi V, Carroll CJ, Auwerx J, et al. Effective treatment of mitochondrial myopathy by nicotinamide riboside, a vitamin B3. EMBO Mol. Med. 2014 n/a – n/a.

Klover P, Chen W, Zhu B-M, Hennighausen L. Skeletal muscle growth and fiber composition in mice are regulated through the transcription factors STAT5a/b: linking growth hormone to the androgen receptor. FASEB J. 2009; 23:3140–3148. [PubMed: 19417088]

Krishnamurthy J, Torrice C, Ramsey MR, Kovalev GI, Al-Regaiey K, Su L, Sharpless NE. Ink4a/Arf expression is a biomarker of aging. J. Clin. Invest. 2004; 114:1299–1307. [PubMed: 15520862]

Kulikova V, Shabalin K, Nerinovski K, Dölle C, Niere M, Yakimov A, Redpath P, Khodorkovskiy M, Migaud ME, Ziegler M, et al. Generation, Release, and Uptake of the NAD Precursor Nicotinic Acid Riboside by Human Cells. J. Biol. Chem. 2015; 290:27124–27137. [PubMed: 26385918]

Lu A, Poddar M, Tang Y, Proto JD, Sohn J, Mu X, Oyster N, Wang B, Huard J. Rapid depletion of muscle progenitor cells in dystrophic mdx/utrophin−/− mice. Hum. Mol. Genet. 2014; 23:4786–4800. [PubMed: 24781208]

Mouchiroud L, Houtkooper RH, Moullan N, Katsyuba E, Ryu D, Cantó C, Mottis A, Jo Y-S, Viswanathan M, Schoonjans K, et al. The NAD(+)/Sirtuin Pathway Modulates Longevity through Activation of Mitochondrial UPR and FOXO Signaling. Cell. 2013; 154:430–441. [PubMed: 23870130]

Pastoret C, Sebille A. Age-related differences in regeneration of dystrophic (mdx) and normal muscle in the mouse. Muscle Nerve. 1995; 18:1147–1154. [PubMed: 7659109]

Revollo JR, Grimm AA, Imai S. The regulation of nicotinamide adenine dinucleotide biosynthesis by Nampt/PBEF/visfatin in mammals. Curr. Opin. Gastroenterol. 2007a; 23:164–170. [PubMed: 17268245]

Revollo JR, Körner A, Mills KF, Satoh A, Wang T, Garten A, Dasgupta B, Sasaki Y, Wolberger C, Townsend RR, et al. Nampt/PBEF/Visfatin regulates insulin secretion in beta cells as a systemic NAD biosynthetic enzyme. Cell Metab. 2007b; 6:363–375. [PubMed: 17983582]

Rongvaux A, Galli M, Denanglaire S, Van Gool F, Drèze PL, Szpirer C, Bureau F, Andris F, Leo O. Nicotinamide phosphoribosyl transferase/pre-B cell colonyenhancing factor/visfatin is required for lymphocyte development and cellular resistance to genotoxic stress. J. Immunol. Baltim. Md. 2008; 1950; 181:4685–4695.

Rybalka E, Timpani CA, Cooke MB, Williams AD, Hayes A. Defects in mitochondrial ATP synthesis in dystrophin-deficient mdx skeletal muscles may be caused by complex I insufficiency. PloS One. 2014; 9:e115763. [PubMed: 25541951]

Sacco A, Mourkioti F, Tran R, Choi J, Llewellyn M, Kraft P, Shkreli M, Delp S, Pomerantz JH, Artandi SE, et al. Short telomeres and stem cell exhaustion model Duchenne muscular dystrophy in mdx/mTR mice. Cell. 2010; 143:1059–1071. [PubMed: 21145579]

Sousa-Victor P, Gutarra S, García-Prat L, Rodriguez-Ubreva J, Ortet L, Ruiz-Bonilla V, Jardí M, Ballestar E, González S, Serrano AL, et al. Geriatric muscle stem cells switch reversible quiescence into senescence. Nature. 2014; 506:316–321. [PubMed: 24522534]

Stein LR, Imai S-I. Specific ablation of Nampt in adult neural stem cells recapitulates their functional defects during aging. EMBO J. 2014

Tan B, Young DA, Lu Z-H, Wang T, Meier TI, Shepard RL, Roth K, Zhai Y, Huss K, Kuo M-S, et al. Pharmacological Inhibition of Nicotinamide Phosphoribosyltransferase (NAMPT), an Enzyme Essential for NAD+ Biosynthesis, in Human Cancer Cells: METABOLIC BASIS AND POTENTIAL CLINICAL IMPLICATIONS. J. Biol. Chem. 2013; 288:3500–3511. [PubMed: 23239881]

Weinstein RS, Hutson MS. Decreased trabecular width and increased trabecular spacing contribute to bone loss with aging. Bone. 1987; 8:137–142. [PubMed: 3606904]

Xu W, Barrientos T, Mao L, Rockman HA, Sauve AA, Andrews NC. Lethal Cardiomyopathy in Mice Lacking Transferrin Receptor in the Heart. Cell Rep. 2015

Yoshino J, Mills KF, Yoon MJ, Imai S. Nicotinamide Mononucleotide, a Key NAD+ Intermediate, Treats the Pathophysiology of Diet- and Age-Induced Diabetes in Mice. Cell Metab. 2011; 14:528–536. [PubMed: 21982712]

Zhao X, Yamazaki D, Park KH, Komazaki S, Tjondrokoesoemo A, Nishi M, Lin P, Hirata Y, Brotto M, Takeshima H, et al. Ca2+ Overload and Sarcoplasmic Reticulum Instability in tric-a Null Skeletal Muscle. J. Biol. Chem. 2010; 285:37370–37376. [PubMed: 20858894]

Highlights

- Mice with ~85% NAD depletion in skeletal muscle are grossly normal as young adults.
- Reduced NAD content impairs mitochondrial function and fiber integrity over time.
- Progressive muscle dysfunction can be reversed by the NAD precursor NR.
- Preventing muscle NAD loss during aging partially preserves exercise performance.

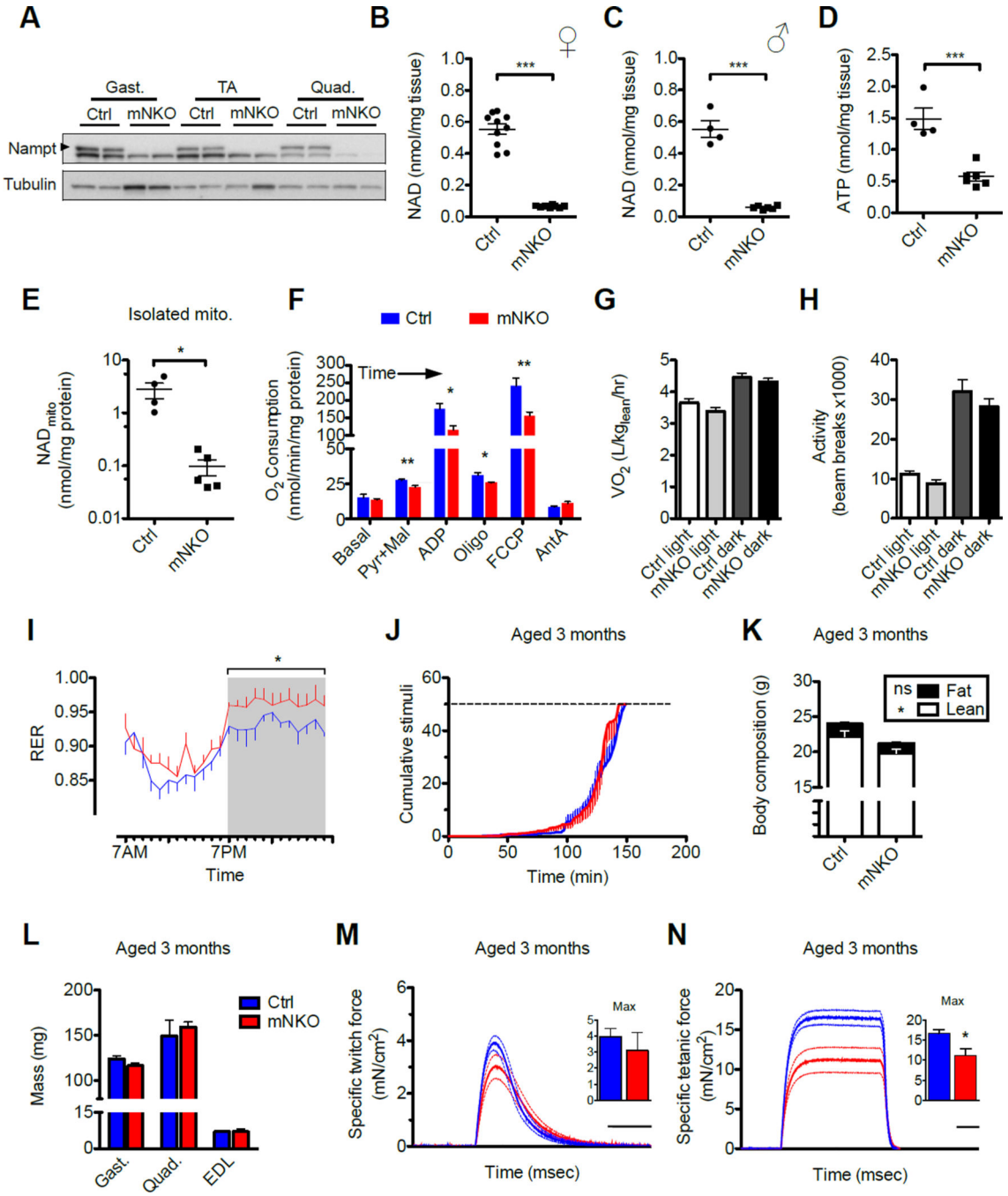

Figure 1. Characterization of mice deficient for Nampt in skeletal muscle

A, Expression of Nampt protein in hindlimb muscles of skeletal muscle-specific Nampt knockout (mNKO) mice compared to floxed littermates. Gastrocnemius (gast.), tibialis anterior (TA), and quadriceps (quad.) of 3-month-old male mice represented.

B, Intramuscular NAD content of hindlimb muscles from female (n=8–10) and

C, Male (n=4–6) mice assessed at 3 months of age.

D, Intramuscular ATP content (n=4–6).

E, NAD content of mitochondria isolated from triceps bracii muscle (n=4–5).

F, Respiratory capacity of isolated muscle mitochondria sequentially provided with pyruvate (pyr), malate (mal), and ADP, followed by complex V inhibitor oligomycin (oligo), uncoupler (FCCP), finally complex III inhibitor antimycin A (AntA) (n=4–6).
G, Mean oxygen consumption (VO_2) normalized to lean body mass (n=7–9) and
H, Voluntary ambulatory activity during light and dark hours (n=8–10).
I, 24-hour time course of respiratory exchange ratio (RER)(n=7–9, *p<0.05).
J, Treadmill running performance (n=6 at baseline). Dashed line indicates exhaustion threshold.
K, Body composition assessed by NMR (n=7–9).
L, Mass of isolated hindlimb muscles (n=6–10).
M, Twitch force and
N, Tetanic force generated by isolated EDL muscle. Dashed lines indicated error bars. Scale bars indicate 100 msec. Inset: maximum force generated per subject (n=4–6). Error bars represent SEM. Significance was determined by Student's t-test (*p<0.05, **p<0.01, ***p<0.001). Mice were 3-month-old males unless otherwise indicated. See also Figure S1.

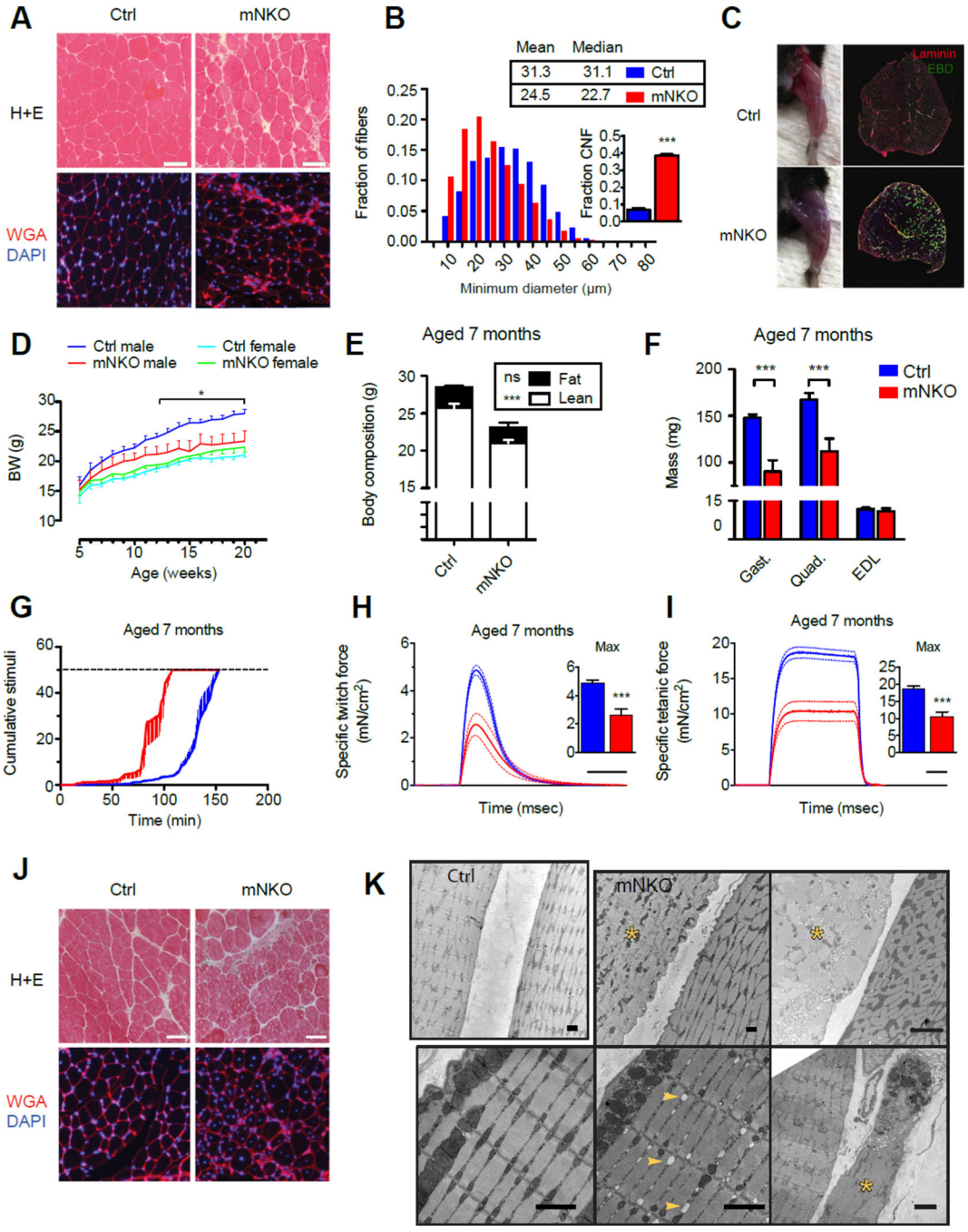

Figure 2. Loss of salvage NAD synthesis results in progressive muscle degeneration

A, Histological sections of EDL muscle from 3-month-old mice stained with H+E or WGA (wheat germ agglutinin) and DAPI to highlight fiber morphology. The scale bar represents 50 µm.

B, Distribution and descriptive statistics of minimum Feret diameters of EDL fibers from 3-month-old mice. Inset: proportion of centrally nucleated fibers (CNF). At least 2.4×10^3 fibers from 3 individuals per group were considered.

C, Representative hindlimb musculature of 3-month-old mice 16 hours after intraperitoneal injection of Evans Blue Dye (EBD). Inset: Histological sections of whole TA muscle stained with laminin and exhibiting fluorescence of EBD.

D, Growth curves from weaning to adulthood (n=7–12 males, 4–15 females).

E, Body composition assessed by NMR at 7 months of age (n=5–10).

F, Mass of isolated male hindlimb muscles at 7 months of age (n=6–10).

G, Treadmill running performance examined at 7 months of age. Dashed line indicates exhaustion threshold (n=6).

H, Twitch force and

I, Tetanic force generated by isolated EDL muscle. Dashed lines indicated error bars. Scale bar indicates 100 msec. Inset: maximum force generated per subject (n=5–10).

J, Histological sections of EDL muscle from 7-month-old mice stained with H+E or WGA and DAPI. The scale bar represents 50 μm.

K, Electron micrographs of EDL muscle taken from female mice aged 7 months. Top left: adjacent fibers in a control muscle. Top middle and top right: A disordered necrotic fiber (yellow asterisk) next to a healthy fiber in an mNKO muscle. Bottom left: Grossly normal fiber morphology in an mNKO muscle. Bottom middle: Pre-necrotic fiber morphology showing swollen sarcoplasmic reticulum (yellow arrows) in an mNKO muscle. Bottom right: Phagocytic cell engulfing debris of a necrotic mNKO fiber (yellow asterisk). Error bars represented SEM. Significance was determined by Student’s t-test (*$p<0.05$,***$p<0.001$). Mice were male unless otherwise indicated. See also Figure S2.

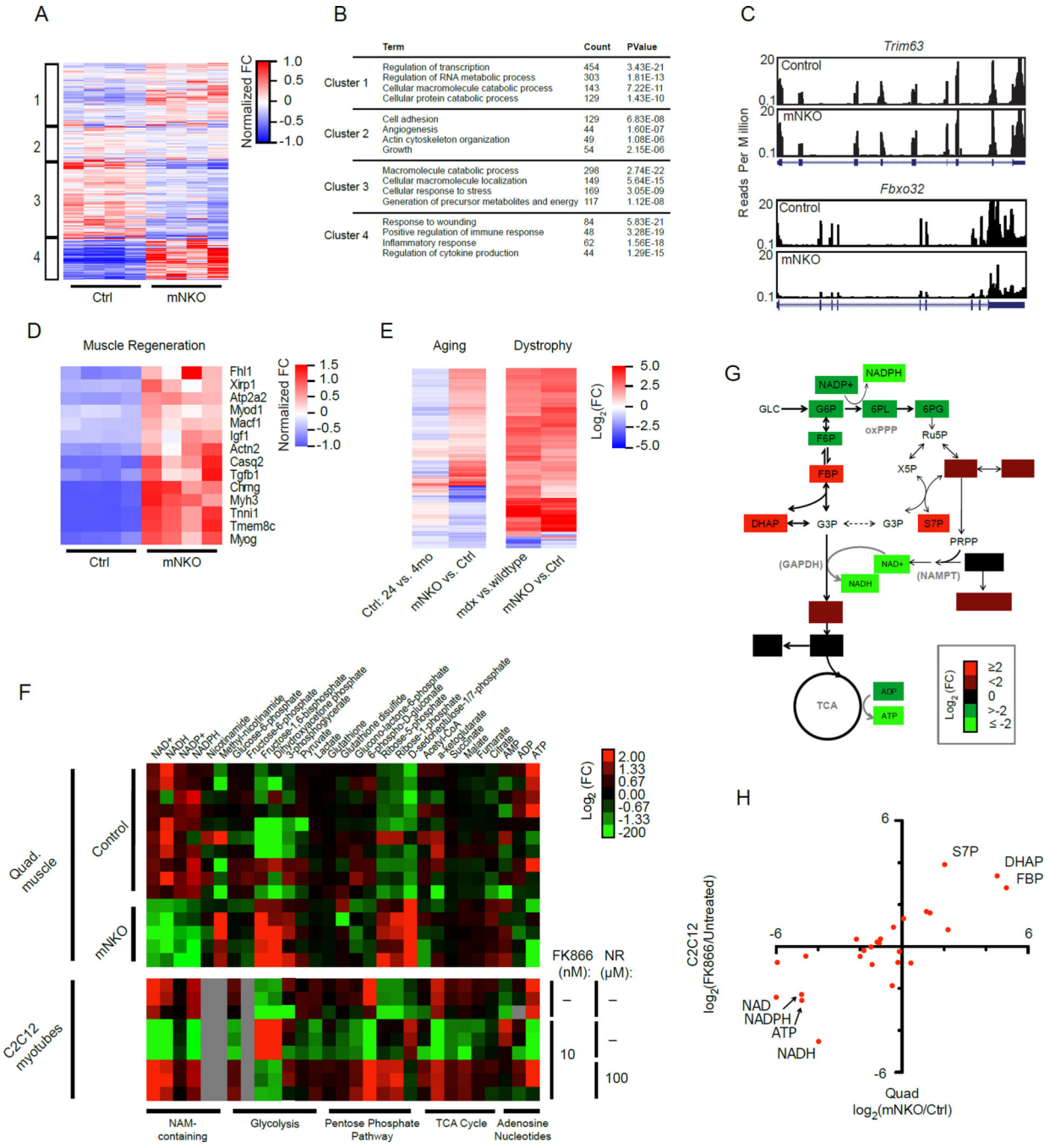

Figure 3. Muscle Nampt deficiency induces pro-inflammatory and regenerative transcriptional programs coincident with alterations in glucose metabolism

A, Heatmap of gene expression in mNKO muscle with each genes assigned to one of four groups according to k-means clustering. Colors indicate fold change (FC) normalized to group means.

B, Selected gene ontology of differentially regulated clusters in B.

C, Coverage of sequencing reads (UCSC browser) for transcripts of the muscle-specific ubiquitin ligases *Trim63* and *Fbxo32*.

D, Heat map of differentially expressed genes relating to muscle regeneration in mNKO.

E, Heatmaps of commonly differentially expressed genes. Left: Control mice aged 24 months vs. 4 months compared to mNKO vs. age-matched controls. Right: The *mdx* model of muscular dystrophy vs. age-matched wildtype controls compared to mNKO vs. age-matched controls. See also Figure S3, S4, and Table S1.

F, Correlation of metabolite abundance between FK866-treated C2C12 myotubes and mNKO quadriceps muscle. Myotubes received 10 nM FK866 for 24 hours.

G, Heatmap indicating relative abundance of metabolites detected in 7-month-old male quadricep muscle (n=5–10) and in C2C12 myotubes treated with 10 nM FK866 and 100 μM NR (n=3), subdivided by metabolic pathway. Grey boxes represent undetected metabolites.

H, Schematic representation of metabolomic analysis in G. Colored metabolites were differentially detected to varying degrees in mNKO muscle while unchanged metabolites did not reach statistical significance. Location of the oxidative pentose phosphate pathway (oxPPP) and the catalytic activity of Nampt and GAPDH are indicated. Mice were male aged 7 months. See also Figure S4.

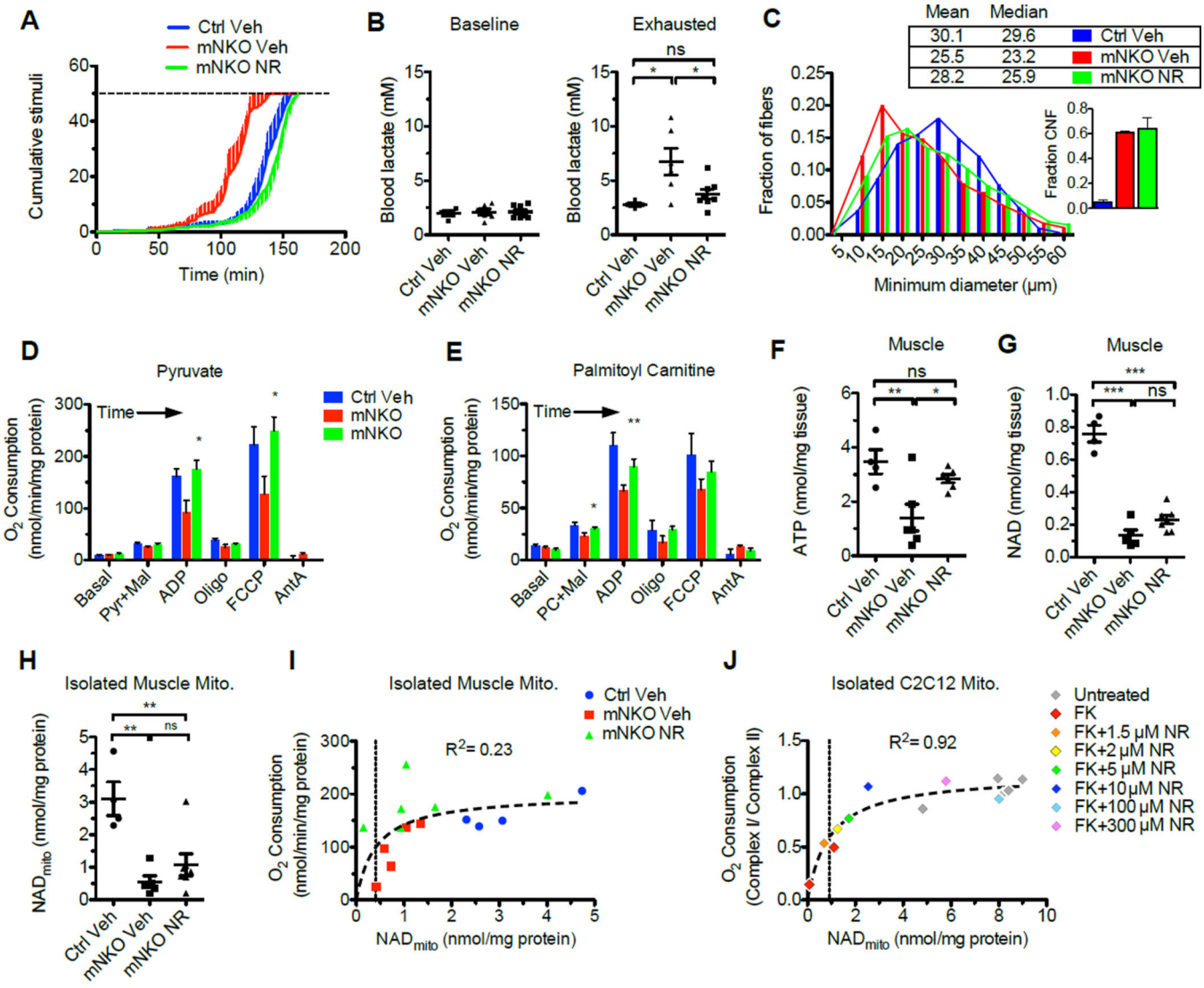

Figure 4. NR ameliorates deficits in mNKO mitochondrial function and fiber morphology

A, Treadmill running performance of 7-month-old mice provided with unsupplemented drinking water (Veh) or NR-supplemented drinking water for 6 weeks and

B, Concentration of blood lactate at baseline and at the point of exercise exhaustion (n=4–8).

C, Distribution and descriptive statistics of minimum Feret diameters of EDL fibers. Inset: proportion of centrally nucleated fibers (CNF). At least 2.0×10^3 fibers from 3 individuals per group were considered.

D, Respiratory capacity of muscle mitochondria provided with excess palmitoyl carnitine or

E, Excess pyruvate (n=4–6, significant changes relative to mNKO Veh).

F, Intramuscular ATP content (n=4–7) in quadriceps muscle following NR treatment.

G, Intramuscular NAD content (n=4–7) and

H, Mitochondrial NAD

I, Relationship between oxygen consumption and NAD content of mitochondria isolated from skeletal muscle (n=4–6). The line indicates a rectangular hyperbolic least squares regression and associated correlation coefficient.

J, Relationship between complex I-dependent respiration and basal NAD content of mitochondria isolated from C2C12 myotubes treated for 24 hours with 10 nM FK866 and 0–300 μM NR. The line indicates a rectangular hyperbolic least squares regression and associated correlation coefficient. Error bars represented SEM. Significance was determined by one-way ANOVA with Tukey's post-hoc test (ns, not significant, *p<0.05,***p<0.001). Mice were female aged 7 months at sacrifice.

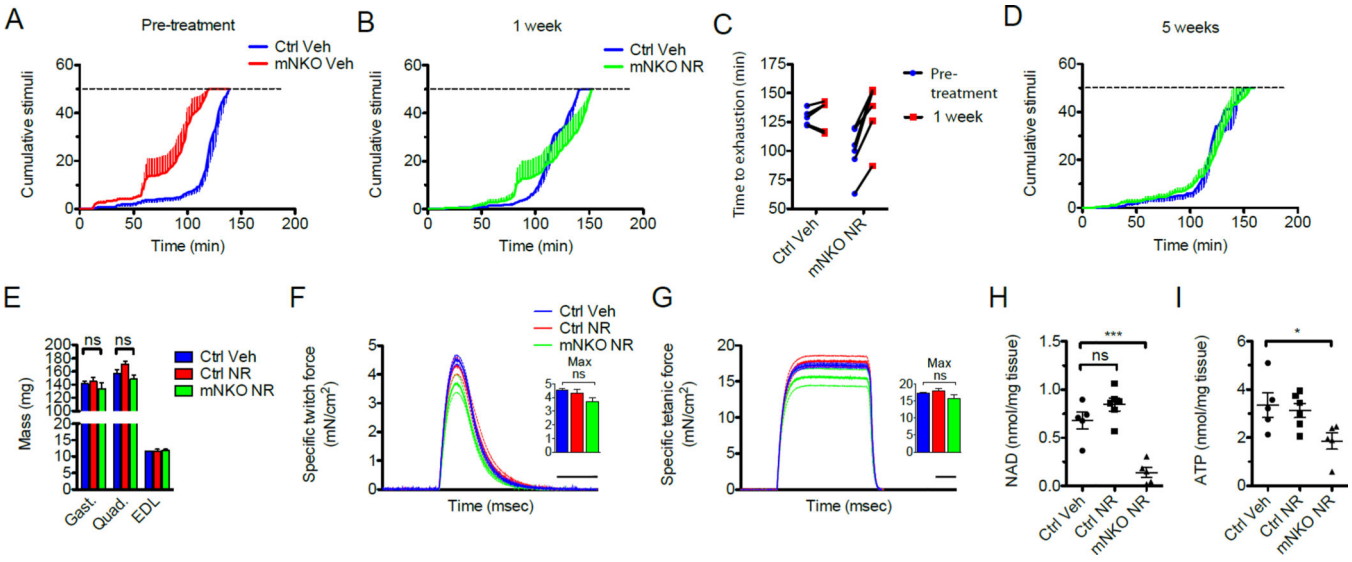

Figure 5. NR reverses deficits in muscle mass, strength, and exercise capacity of mNKO mice

A, Treadmill performance of 5.5-month-old mice before beginning NR administration (n=5–6).

B, Treadmill performance after 1 week of treatment and

C, Change in exhaustion time of individual mice at the point of exhaustion across the first week of treatment (n=5–6).

D, Treadmill performance after 5 weeks of NR treatment (n=5).

E, Mass of hindlimb muscles isolated after 6 weeks of NR administration (n=5–6).

F, Twitch force and

G, Tetanic force generated by isolated EDL muscle. Dashed lines indicated error bars. Scale bars indicate 100 msec. Insets: maximum force generated per subject (n=5–6).

H, Intramuscular NAD content and

I, Intramuscular ATP content assessed in quadriceps after 6 weeks of treatment (n=5–6). Error bars represented SEM. Significance was determined by one-way ANOVA with Tukey's post-hoc test (ns, not significant, *p<0.05,***p<0.001). Mice were male aged 7 months at sacrifice. See also Figures S5 and S6.

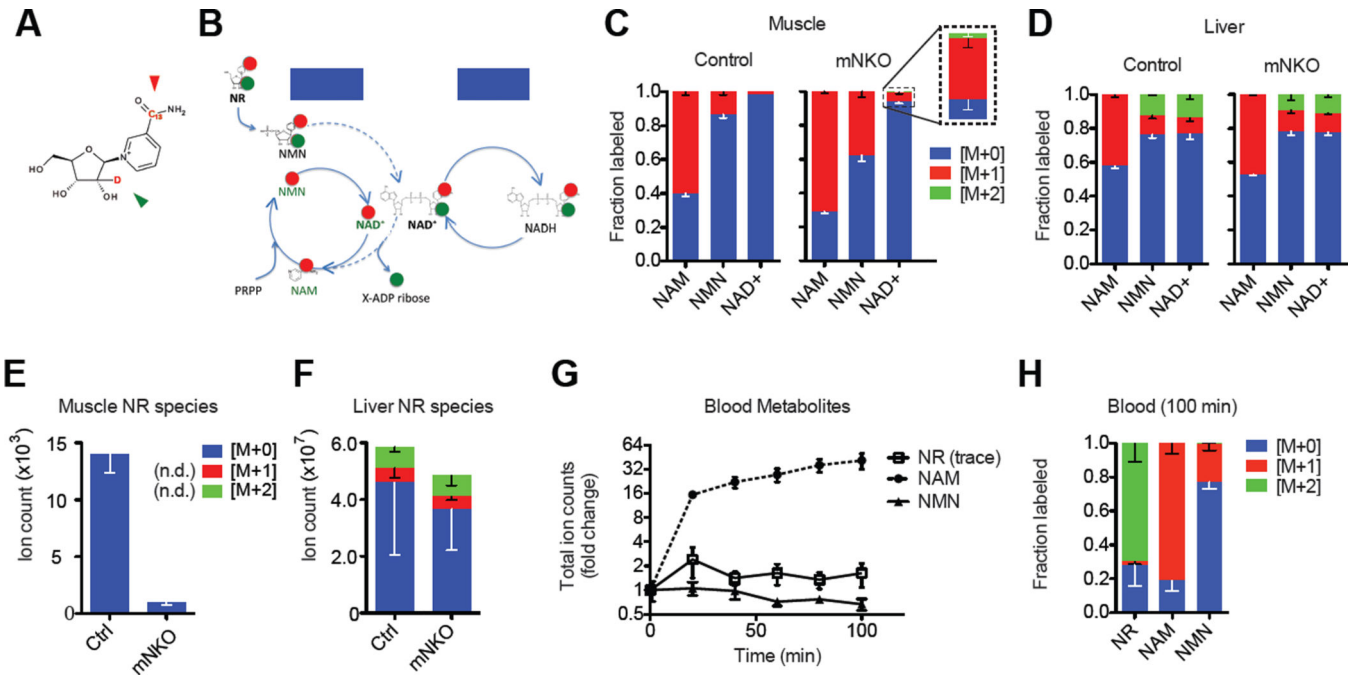

Figure 6. Oral bioavailability of NR to muscle

A, Molecular structure of the NR^{M+2} mass isotopologue. Green and red arrows indicate locations of ^{13}C and deuterium labels, respectively.

B, Schematic of proposed NR^{M+2} entry into the NAD salvage pathway (dashed lines, ATP omitted) and the subsequent separation of the isotopes on ribose and NAM moieties. Basal metabolic redox processes do not affect the arrangement of the labels.

C, Incorporation pattern of heavy isotopes into intermediates of the NAD salvage pathway in skeletal muscle and

D, Liver tissue 100 minutes after oral gavage with 200 mg/kg NR^{M+2} (n=3).

E, Detection of NR isotopologues in quadriceps muscle and

F, Liver tissue 100 minutes after oral gavage with 200 mg/kg NR^{M+2}. Some isotopologues were not detected (n.d.) in muscle (n=3).

G, Appearance of blood metabolites after oral gavage with 200 mg/kg NR^{M+2} and

H, Fractional labeling in blood after 100 minutes (n=3 per genotype, pooled). NR was detected in trace amounts. Error bars represented SEM. Significance was determined by one-way ANOVA with Tukey's post-hoc test (ns, not significant, *p<0.05,**p<0.01). Mice were female aged 7 months.

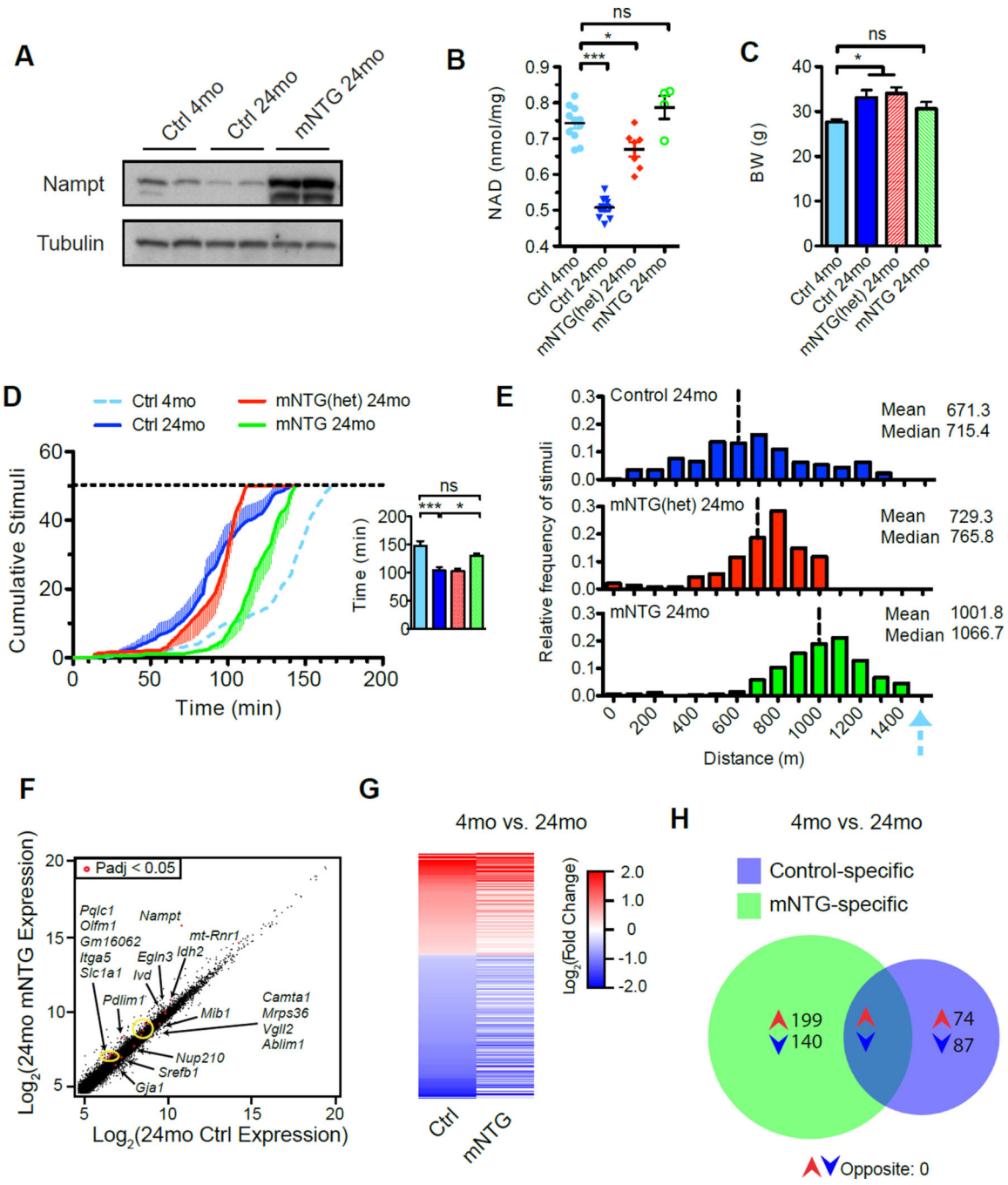

Figure 7. Lifelong elevation of muscle Nampt expression increases exercise capacity of aged mice

A, Expression of exogenous Nampt protein persists in muscle until 24 months of age.

B, Age-related alterations in intramuscular NAD content assessed in gastrocnemius muscle of 4-month-old (4 mo) and 24-month-old (24 mo) mice with one ($mNTG^{het}$) or two (mNTG) copies of the *Nampt* transgene (n=4–11).

C, Body weights of old mice were moderately affected by the transgene (n=7–14).

D, Treadmill performance in 24-month-old mice. Horizontal dashed line indicates the exhaustion threshold. The blue dashed line indicates the performance of young control littermates. Inset: time elapsed at the point of exhaustion (n=7–14).

E, Histogram and descriptive statistics of stimuli received by group and binned by running distance at the point of exhaustion, as described in D. Vertical dashed lines indicate group means. The blue arrow indicates the mean running distance of young control littermates.

F, Correlation plot representing RNAseq gene expression profiling in quadricep muscle in 24-month-old mice (n=3–5). Labeled red dots indicate significant differences in expression (Padj, adjusted p-value) with associated gene names indicated.

G, Heatmap of relative gene expression reveals negligible impact of sustained NAD salvage on transcriptional programs of muscle with age. Genes in mNTG are presented based on significant differences in expression between controls aged 4 vs. 24 months.

H, Overlap in differentially regulated genes of control and mNTG muscle between 4 and 24 months of age. There were no significantly opposing transcripts between the genotypes.

Young control data are reproduced from previously published results (Frederick et al., 2015). Error bars represented SEM. Significance was determined by one-way ANOVA with Tukey's post-hoc test (ns, not significant, *$p<0.05$,***$p<0.001$). Mice were male of respective ages. See also Table S2.